

## Effect of WO<sub>3</sub> Nanoparticles on Congo Red and Rhodamine B Photo Degradation

**Alaei, Mahshad\***<sup>+</sup>

Nanotechnology Research Center, Research Institute of Petroleum Industry (RIPI),  
P.O. Box 14665-1998 Tehran, I.R. IRAN

**Mahjoub, Ali Reza**

Department of Chemistry, Faculty of Science, Tarbiat Modares University (TMU),  
P.O. Box 14115-336 Tehran, I.R. IRAN

**Rashidi, Alimorad**

Nanotechnology Research Center, Research Institute of Petroleum Industry (RIPI),  
P.O. Box 14665-1998 Tehran, I.R. IRAN

**ABSTRACT:** Tungsten trioxide nanoparticles with two different sizes (average particle sizes about 50 and 80 nm) were prepared by the spray pyrolysis method. Photo degradation of Congo Red (azo dye) showed that photo catalytic property of the as-prepared WO<sub>3</sub> nanoparticles with average size about 80 nm is higher than the sample with average size about 50 nm. Photo degradation of Rhodamine B (cationic triarylmethane dye) showed that photo catalytic property of the as-prepared WO<sub>3</sub> nanoparticles with average size about 50 nm is higher than the sample with average size about 80 nm. The samples were characterized with X-Ray Diffraction (XRD), Scanning Electron Microscopy (SEM), EDX analysis and UV-visible spectrum. Different interactions between dyes and the photo catalyst surface, probably causes the inverse behavior of WO<sub>3</sub> nanoparticles with two different sizes in Congo Red and Rhodamine B photo degradation reactions.

**KEY WORDS:** WO<sub>3</sub> nanoparticles, Photo degradation, Rhodamine B, Congo Red.

### INTRODUCTION

Numerous industries such as cosmetics, paper, food and textiles use dye in order to colorise their products. Some of these dyes and their degradation products such as aromatic amines are highly carcinogenic and dangerous. Even at very low concentration, the presence of these dyes in water is highly visible.

One of the advanced oxidation processes (AOPs) is heterogeneous photo catalysis that is an efficient waste water treatment technique used for the total mineralization of organics [1,2].

WO<sub>3</sub> is a wide band gap semiconductor with interesting photo catalytic properties that has potential

---

\* To whom correspondence should be addressed.

+ E-mail: [alaiem@ripi.ir](mailto:alaiem@ripi.ir)

1021-9986/12/1/23

7/5/2.70

applications for solar energy and electro chromic devices [3-5], catalysts and gas sensors [6-8].

Various methods including chemical vapor deposition [9], electrochemical deposition [10], sol-gel coating [11-13] and electrochemical anodization [14] have been reported for the fabrication of tungsten oxide nanostructures. The spray pyrolysis technique for material synthesis is economical method and an interesting option due to the use of inexpensive precursor materials, low-cost equipments and its relative ease in preparing the large scale of nanomaterials.

In this work, two different sizes of  $\text{WO}_3$  nanoparticles were prepared.  $\text{WO}_3$  nanoparticles that were prepared with spray pyrolysis method are spherical shape with an average size about 80 and 50 nm. The as-prepared samples were used as photo catalyst in Congo Red (azo dye) and Rhodamin B (cationic triarylmethane dye) photo degradation.

## EXPERIMENTAL SECTION

### Materials

All chemicals were of analytical grade and used without further purification.

### Preparation of $\text{WO}_3$ nanoparticles

The spray process was done with a stainless-steel atomizer. Aqueous solution of ammonium para tungstate (for example 1.6 wt %) together a suitable organic additive (such as citric acid) was sprayed to the vertical furnace by using compressed air as carrier gas. The solution pH was adjusted at 3 and 9 for preparing  $\text{WO}_3$  nanoparticles with average size about 50 and 80 nm respectively.

### Photo degradation reactions

The degradations were carried out at 293 K. 100 mL Congo Red aqueous solution (5 ppm) or Rhodamine B (1 ppm) together with 0.1 g photo catalyst was illuminated with UV radiation in the presence of the air bubbles. UV-irradiation (365 nm) was provided by a high pressure mercury lamp (Philips HPK-125W). Each 30 min., 4 mL sample was separated, centrifuged for removal of catalyst and characterized with UV-visible spectrometer.

### Characterization

The samples were characterized by scanning electron microscopy (SEM) using a Holland Phillips XL30 microscope. XRD patterns of the sample were recorded in ambient air using a Holland Phillips X-ray power

diffraction (Cu  $K\alpha$ ,  $\lambda=1.5406 \text{ \AA}$ ), at scanning speed of  $2^\circ/\text{min}$  from  $20^\circ$  to  $80^\circ$ . UV-visible spectrums were prepared by Shimadzu analytical equipment (UV-2100).

## RESULTS AND DISCUSSIONS

### Preparation of $\text{WO}_3$ nanoparticles

SEM image was used to investigate the microscopic structure of the samples. Fig. 1(a) and 1(b) illustrates the SEM data from nanoparticles at two different pH. SEM images show that the most particles of the samples are spherical shape.

In order to find chemical composition of the particles, EDX analyze was carried out. Fig. 1(c) shows the EDX analysis of the  $\text{WO}_3$  nanoparticles that was prepared by spray pyrolysis method at pH=9. It was observed just W atom with no remarkable impurity. An XRD analysis was carried out to discover the crystalline phase and structure of the  $\text{WO}_3$  nanoparticles.

The results for both samples shows the formation of tungsten trioxide with monoclinic structure which is depicted in Fig. 2. The obtained spectrum has the first three  $\text{WO}_3$  main peaks at  $2\theta = 23.1, 24.4, 26.6$ , in good agreement with the JCPDS 05-0363 standard card. The average particle size of the products was calculated from XRD pattern by the Debye-Scherrer formula is about 50 and 80 nm respectively.

### Photo degradation reactions

The photo catalytic activity of  $\text{WO}_3$  nanoparticles was measured by photo degradation of Congo Red (CR) and Rhodamine B (RB) under UV irradiation.

By applying the following simple first-order rate law,  $-\ln(C/C_0) = kt$  (based on Beer-Lambert law), to the results of the current study, a linear relationship between  $-\ln(C/C_0)$  and time (t), which was consistent with the first-order kinetics was observed. Each plot was determined at the maximum absorbance of each dye.

UV-visible spectrums of Congo Red absorption ( $\lambda = 510 \text{ nm}$ ) and Rhodamine B absorption ( $\lambda = 540 \text{ nm}$ ) in the presence of two samples of the as-prepared  $\text{WO}_3$  nanoparticles with different average particle sizes illustrates in Fig. 3. It was observed that by increasing the irradiation time, the maximum absorption peak decreases, which means that the concentration of Congo Red or Rhodamine B is decreasing in the presence of  $\text{WO}_3$  nanoparticles and UV illumination. The photo

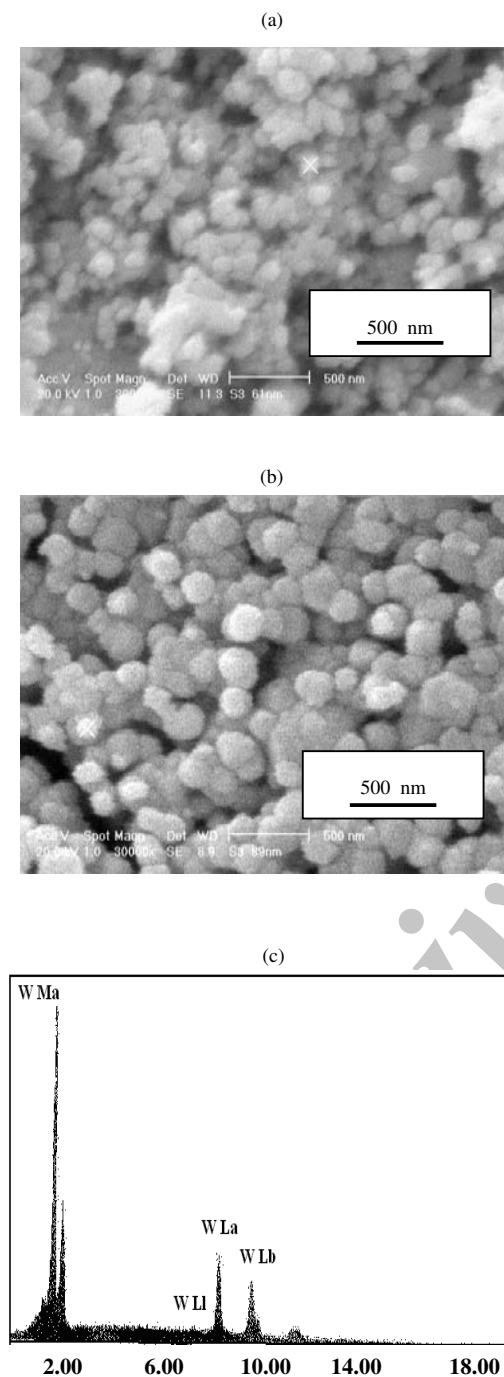


**Fig. 1:** SEM images of the as-prepared  $\text{WO}_3$  nanoparticles that was prepared by spray pyrolysis method in different pH (a:pH=3, b:pH=9) c: EDX analysis of the as-prepared  $\text{WO}_3$  nanoparticles that was prepared by spray pyrolysis method at pH=9.

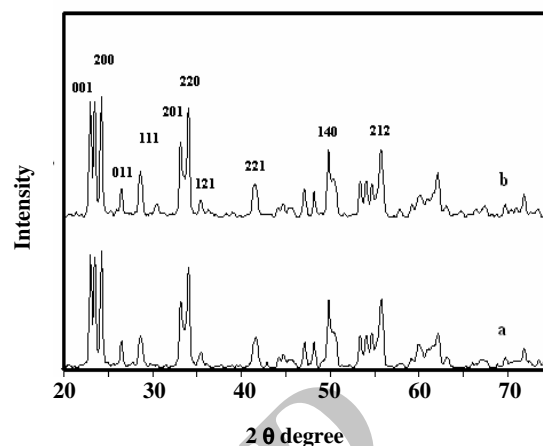


**Fig. 2:** XRD patterns of  $\text{WO}_3$  nanoparticles that were prepared by spray pyrolysis method in different pH (a: pH=3, b: pH=9) that is indicated monoclinic structure for both samples.

degradation rates of the both reactions are compared in Fig. 4(a) and Fig. 4(b). In the case of Congo Red photo degradation, photo catalytic property of  $\text{WO}_3$  nanoparticles with average size about 80 nm is higher than  $\text{WO}_3$  nanoparticles with average size about 50 nm but this property is inverse for the mentioned samples in the case of Rhodamine B photo degradation.

The chemical structure of Congo Red (azo dye) and Rhodamine B (cationic triarylmethane) was illustrated in the Fig. 5(a) and 5(b). The zero point charge for  $\text{WO}_3$  is 1-1.5 [15] and above this value, the  $\text{WO}_3$  surface is predominantly negatively charged when the pH is higher than the  $\text{WO}_3$  isoelectric point. These photo degradation reactions occurred at pH 5.5 that is above the isoelectric point of  $\text{WO}_3$ . More efficient formation of hydroxyl radical occurs in this condition and the  $\text{WO}_3$  surface is negatively charged and Rhodamine B was adsorbed onto the  $\text{WO}_3$  surface through the positive ammonium groups while the negatively charged surface repels Congo Red  $\text{R-SO}_3^-$  ions. Besides, the large steric hindrance due to large aromatic ensembles, including one central biphenyl group and two symmetric naphthalenic groups in the Congo Red chemical structure causes less interaction with surface of  $\text{WO}_3$  nanoparticles in comparison to Rhodamine B [16]. The reaction rate diagrams that are represented in Fig. 4 are in agreement to these matters. On the other hand, surface area of the as-prepared  $\text{WO}_3$  nanoparticles with average size about 50 nm is higher than  $\text{WO}_3$  nanoparticles with average size about 80 nm.

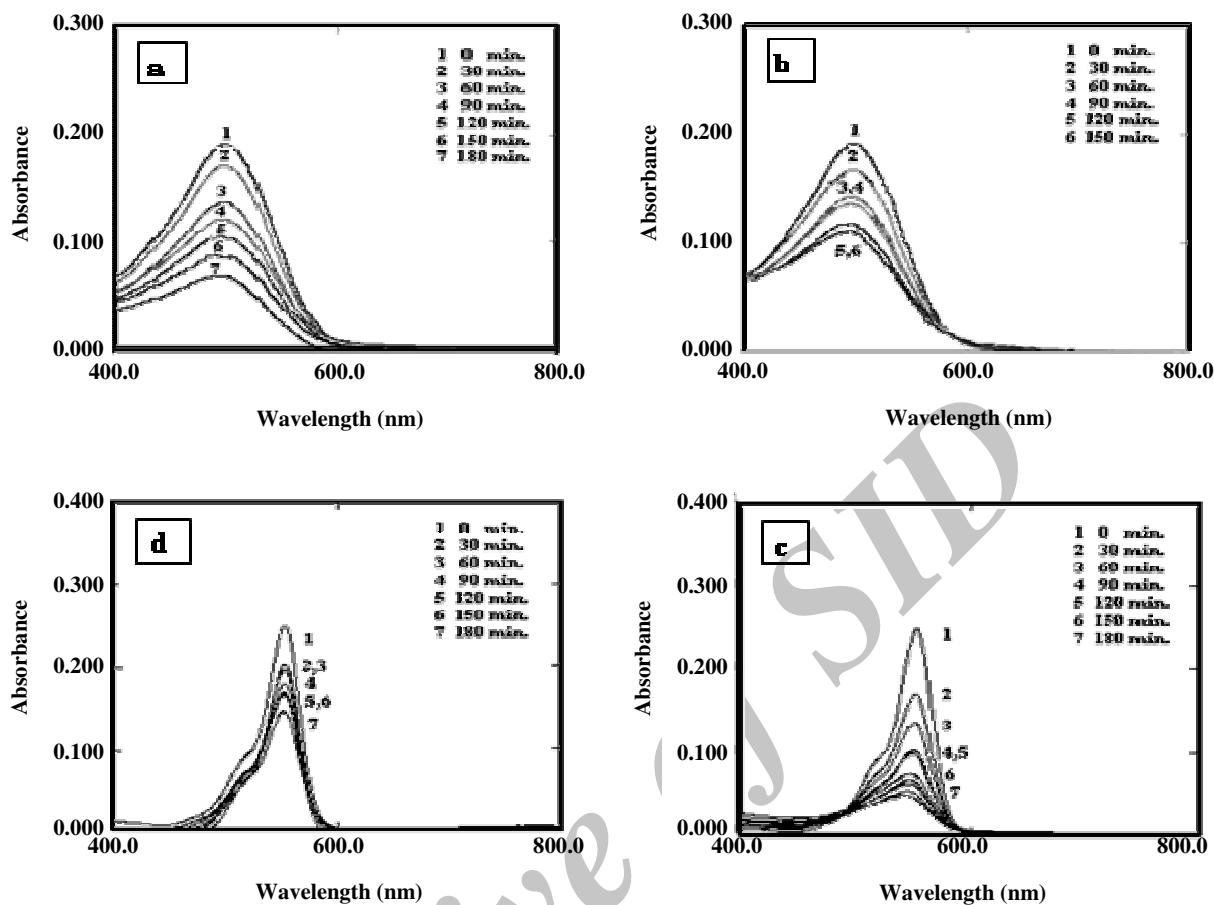


Fig. 3: Evaluation of  $WO_3$  nanoparticles photo catalytic activity by photo degradation of a: Congo Red aqueous solution together  $WO_3$  nanoparticles with average size about 80 nm. b: Congo Red aqueous solution together  $WO_3$  nanoparticles with average size about 50 nm. c: Rhodamine B aqueous solution together  $WO_3$  nanoparticles with average size about 80 nm. d: Rhodamine B aqueous solution together  $WO_3$  nanoparticles with average size about 50 nm.

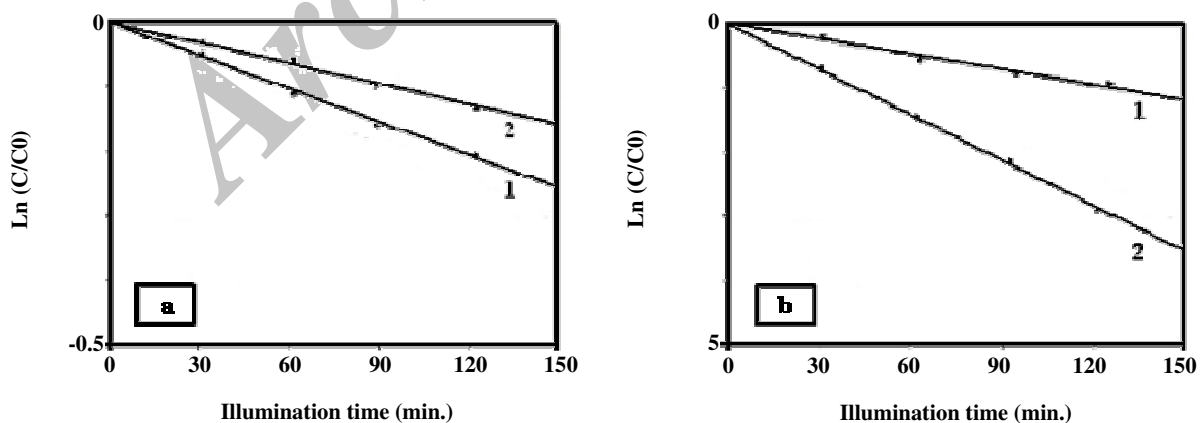


Figure 4. The photo degradation rate of (a) Congo Red aqueous solution (b) Rodamine B aqueous solution in the presence of the as-prepared  $WO_3$  nanoparticles with average size about (1) 80 nm (2) 50 nm.

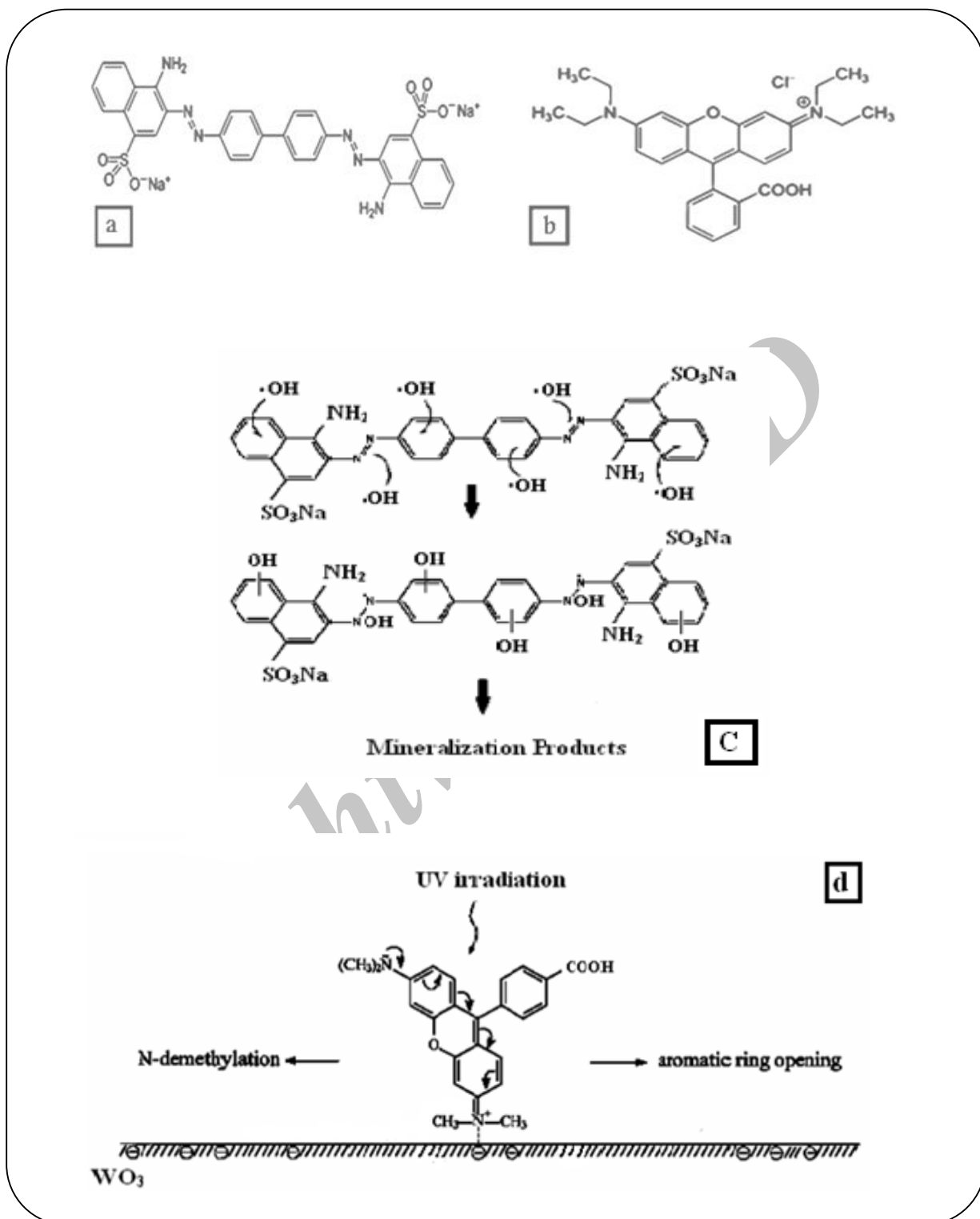


Fig. 5: Chemical structure of a: Congo Red (azo dye) and b: Rhodamine B (cationic triarylmethane) c: Proposed mechanism of Congo Red photo degradation mechanism UV irradiation in aqueous  $\text{WO}_3$  nanoparticles dispersions. d: Proposed mechanism of Rhodamine B photo degradation mechanism UV irradiation in aqueous  $\text{WO}_3$  nanoparticles dispersions.

Therefore the amount of the negative charge in surface unit of the first mentioned sample is more than the other sample. According to the Fig. 5(b), Rhodamine B has positive charge that can have better interaction with WO<sub>3</sub> nanoparticles with smaller particle size.

Fig. 5(c) and 5(d), represents the proposed mechanism schematically for photo degradation of Congo Red and Rhodamine B under UV irradiation respectively. Fig. 5(d) shows an adsorption model in which the WO<sub>3</sub> surface negatively charged and the Rhodamine B adsorbed on the WO<sub>3</sub> surface through the positive ammonium groups.

Our proposed mechanism for the photo degradation of the desired dyes at pH 5.5 is as follows.

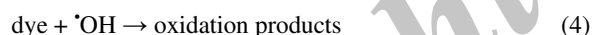
Under UV irradiation, most of the  $\cdot\text{OH}$  radicals are generated directly from the reaction between the holes and surface adsorbed H<sub>2</sub>O or  $\text{OH}^-$ . O<sub>2</sub><sup>-</sup> should be much less likely form than  $\cdot\text{OH}$  [17]. Therefore we can consider the following equations.



While some electron-hole pairs are recombined, the remaining holes generate  $\cdot\text{OH}$  radicals either with adsorbed water (2) or with adsorbed  $\text{OH}^-$  (3).



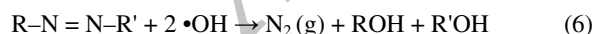
$\cdot\text{OH}$  radical is a strong oxidant for the complete mineralization of organic chemicals.



$h^+$  may act as oxidant, especially at high concentration



As revealed by various studies on the photo degradation of azo dyes such as Congo Red, the chromophore azo group is easily broken to generate N<sub>2</sub> gas:



Also Congo Red was oxidized by oxidative species and converted into fatty acids and finally into CO<sub>2</sub>. Among the oxidative species,  $\cdot\text{OH}$  is the major oxidative transient and is known to react with benzene and azo moieties with high rate coefficients [18].

The resulting intermediates are degraded progressively through hydroxylation of aromatic rings by  $\cdot\text{OH}$ , ring openings and photo-Kolbe decarboxylation reactions until total mineralization [19-21].

## CONCLUSIONS

In this research, WO<sub>3</sub> nanoparticles with different average particle sizes (50 nm and 80 nm) were prepared by spray pyrolysis method. SEM images demonstrate uniform nanoparticles. XRD patterns illustrate the formation of WO<sub>3</sub> phase with monoclinic structure. The photocatalytic activity of WO<sub>3</sub> nanoparticles were measured by photo degradation of Congo Red (azo dye) and Rhodamine B (cationic tri aryl methane dye) under UV irradiation. The results show that in the case of Congo Red photo degradation, by increasing the average particle size, photocatalytic property of the as-prepared WO<sub>3</sub> nanoparticles will be increased while in the case of Rhodamine B photo degradation, smaller particle size of the desired photocatalyst will be more active than the other sample.

Received : Sep. 9, 2010 ; Accepted : May 16, 2011

## REFERENCES

- [1] Mills A., Lee S.K., A Web-Based Overview of Semiconductor Photochemistry-Based Current Commercial Applications, *J. Photochem. Photobiol. A: Chem.*, **152**, p. 233 (2002).
- [2] Hoffmann M.R., Martin S.T., Choi W., Behnemann D.W., Environmental Applications of Semiconductor Photocatalysis, *Chem. Rev.*, **95**, p. 69 (1995).
- [3] Bellac D.L., Azens A., Granqvist C.G., Angular Selective Transmittance Through Electrochromic Tungsten Oxide Films Made by Oblique Angle Sputtering, *Appl. Phys. Lett.*, **66**, p. 1715 (1995).
- [4] Jelle B.P., Hagen G., Performance of an Electrochromic Window Based on Polyaniline, Prussian Blue and Tungsten Oxide, *Sol. Energy Mater. Sol. Cells*, **58**, p. 277 (1999).
- [5] Turyan I., Krasovec U.O., Orel B., Saraidorov T., Reisfeld R., Mandler D., "Writing-Reading-Erasing" on Tungsten Oxide Films Using the Scanning Electrochemical Microscope, *Adv. Mater.*, **12**, p. 330 (2000).
- [6] Chaudhari G.N., Bende A.M., Bodade A.B., Patil S.S., Sapkal V.S., Structural and Gas Sensing Properties of Nanocrystalline TiO<sub>2</sub>:WO<sub>3</sub>-Based Hydrogen Sensors, *Sens. Actuators B*, **115**, p. 297 (2006).
- [7] Morandi S., Ghiotti G., Chiorino A., Bonelli B., Comini E., Sberveglieri G., MoO<sub>3</sub>-WO<sub>3</sub> Mixed Oxide Powder and Thin Films for Gas Sensing Devices: A Spectroscopic Characterisation, *Sens. Actuators B*, **28**, p. 111 (2005).

- [8] Guidi V., Blo M., Butturi M.A., Carotta M.C., Galliera S., Giberti A., Malagù C., Martinelli G., Piga M., Sacerdoti M., Vendemiati B., Aqueous and Alcoholic Syntheses of Tungsten Trioxide Powders for NO<sub>2</sub> detection, *Sens. Actuators B*, **100**, p. 277 (2004).
- [9] Brescacin E., Basato M., Tondello E., Amorphous WO<sub>3</sub> Films via Chemical Vapor Deposition from Metallorganic Precursors Containing Phosphorus Dopant, *Chem. Mater.*, **11**, p. 314 (1999).
- [10] Yu Z.R., Jia X.D., Du J.H., Zhang J.Y., Electrochromic WO<sub>3</sub> Films Prepared by a New Electrodeposition Method, *Sol. Energy Mater. Sol. Cells*, **64**, p. 55 (2000).
- [11] Aliev A.E., Shin H.W., Nanostructured Materials for Electrochromic Devices, *Solid State Ion.*, **154-155**, p. 425 (2002).
- [12] Badilescu S., Ashrit P.V., Study of Sol-Gel Prepared Nanostructured WO<sub>3</sub> Thin Films and Composites for Electrochromic Applications, *Solid State Ion.*, **158**, p. 187 (2003).
- [13] Ozkan E., Lee S., Liu P., Tracy C.E., Tepehan F.Z., Pitts J.R., Deb S.K., Electrochromic and Optical Properties of Mesoporous Tungsten Oxide Films, *Solid State Ion.*, **149**, p. 139 (2002).
- [14] Tsuchiya H., Macak J.M., Sieber I., Taveira L., Ghicov A., Sirotna K., Schmuki P., Self-Organized Porous WO<sub>3</sub> Formed in NaF Electrolytes, *Electrochem. Commun.*, **7**, p. 295 (2005).
- [15] Veith G.M., Lupini A.R., Pennycook S.J., Villa A., Prati L., Dudney N.J., Magnetron Sputtering of Gold Nanoparticles onto WO<sub>3</sub> and Activated Carbon, *Catal. Today*, **122**, p. 248 (2007).
- [16] Lachheb H., Puzenat E., Houas A., Ksibi M., Elimame Elaloui, Guillard C., Herrmann J., Photocatalytic Degradation of Various Types of Dyes (Alizarin S, Crocein Orange G, Methyl Red, Congo Red, Methylene Blue) in Water by UV-Irradiated Titania, Photocatalytic Degradation of Various Types of Dyes (Alizarin S, Crocein Orange G, Methyl Red, Congo Red, Methylene Blue) in Water by UV-Irradiated Titania, *Appl. Catal. B: Environ.*, **39**, p. 75 (2002).
- [17] Fernandez J., Kiwi M., Lizama C., Freer J., Baeza J., Mansilla H.D., Factorial Experimental Design of Orange II Photocatalytic Discolouration, *J. Photochem. Photobiol. A*, **151**, p. 213 (2002).
- [18] Ma H., Wang M., Yang R., Wang W., Zhao J., Shen Z., Yao S., Radiation Degradation of Congo Red in Aqueous Solution, *Chemosphere*, **68**, p. 1098 (2007).
- [19] Akyol A., Bayramoglu M., The Degradation of an Azo Dye in a Batch Slurry Photocatalytic Reactor, *Chem. Eng. Proc.*, **47**, p. 2150 (2008).
- [20] Alaei M., Rashidi A.M., Mahjoub A., Two Suitable Methods for the Preparation of Inorganic Fullerene-Like (IF) WS<sub>2</sub> Nanoparticles, *Iran. J. Chem. Chem. Eng. (IJCCE)*, **50**, p. 91 (2009).
- [21] Sharbatdaran M., Novinrooz A., Noorkojouri H., Preparation and Characterization of WO<sub>3</sub> Electrochromic Films Obtained by the Sol - Gel Process, *Iran. J. Chem. Chem. Eng.*, **38**, p. 25 (2006).